Contribution from the Chemical Physics Program, Washington State University, Pullman, Washington 99164, and the Groupe des Transitions de Phases, CNRS, Grenoble, France

Structure and Magnetic Properties of Two Two-Dimensional Copper Oxalates: $(C_6H_5CH_2NH_3)_2Cu(C_2O_4)_2$ and $(NH_3C_3H_6NH_3)Cu(C_2O_4)_2$

D. R. BLOOMQUIST, J. J. HANSEN, C. P. LANDEE, R. D. WILLETT,* and R. BUDER

Received July 17, 1980

The crystal structures of bis(benzylammonium) bis(oxalato)cuprate(II), $(C_6H_5CH_2NH_3)_2Cu(C_2O_4)_2$ ($(BA)_2Cu(ox)_2$), and propylenediammonium bis(oxalato)cuprate(II), $(C_3H_6N_2H_6)Cu(C_2O_4)_2$($(PDA)Cu(ox)_2$), ($(PDA)Cu(ox)_2$), have been determined, and the magnetic susceptibilities of the compounds have been measured from 4 to 300 K. $(BA)_2Cu(ox)_2$ belongs to the orthorhombic space group *Pbca* with a = 7.100 (2) Å, b = 8.004 (2) Å, and c = 35.444 (8) Å while $(PDA)Cu(ox)_2$ is monoclinic, $C2/c$, with a = 17.901 (3) Å, b = 4.920 (1) Å, c = 14.002 (3) Å, and β = 118.7 (2)°. Each salt contains essentially planar $Cu(ox)_2^{2-}$ anions, which aggregate to form chain- (PDA) or layer-type (BA) structures. In $(BA)_2Cu(ox)_2$, the $Cu(ox)_2^{2-}$ anions stack in a centered rectangular array in the *ab* plane, with long interion Cu–O interactions between ions stabilizing the layer structure. The two-dimensional layers are separated by the benzylammonium cations and display antiferromagnetic interactions with J/k = –0.21 K. $(PDA)Cu(ox)_2$ contains one-dimensional chains of the $Cu(ox)_2^{2-}$ anions parallel to the *b* axis with pairs of long Cu–O bonds between anions. The PDA ions hydrogen bond adjacent chains together, forming sheets in the *bc* plane. The magnetic data for $(PDA)Cu(ox)_2$ can be fit to a ferromagnetic $S = {}^1/_2$ one-dimensional model (J/k = 19 K). Strong antiferromagnetic coupling between chains also exists (J'/k = –11 K).

Introduction

There has been considerable recent interest in magnetic superexchange pathways that involve the oxalate ion, primarily due to the unusually strong antiferromagnetic interactions that occur in $Cu(ox)\cdot{}^1/_3H_2O$.[1-3] This amorphous material behaves as a linear chain system with J = –291 cm^{-1} (J/k = –419 K).[4] A recent EXAFS study revealed[5] that the oxalate ion acted as a double bidentate ligand, coordinating to two copper ions as in **1**. Each copper ion has a square-planar coordination

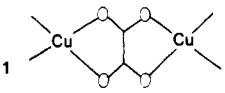

1

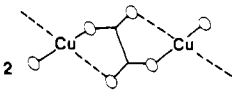

2

geometry, with adjacent copper ions bridged by a single oxalate ion. The unpaired electrons in the $d_{x^2-y^2}$ orbitals on adjacent copper ions interact with the σ framework on the oxalate ion in a nonorthogonal manner.[6] Thus strong antiferromagnetic coupling is observed. In $Cu(ox)(NH_3)_2\cdot 2H_2O$, on the other hand, a linear chain structure is formed in which the bridging oxalate ions coordinate in a monodentate fashion (the elongated coordination sites are occupied by the other oxygen atoms of the oxalates)[7] as in **2**. The unpaired electrons from the $d_{x^2-y^2}$ orbitals on adjacent copper ions now interact in a nearly orthogonal fashion, and the exchange coupling is much weaker (J = –11.9 cm^{-1}; J/k = –17.1 K).

As part of a continuing study in this laboratory of two-dimensional magnetic systems, the salt $(BA)_2Cu(ox)_2$ (BA = $C_6H_5CH_2NH_3^+$, ox = $C_2O_4^{2-}$) was prepared. It was anticipated that this compound would display low-dimensional magnetic behavior analogous to that previously studied in salts of the form $(A)_2Cu(X)_4$ where A is a substituted ammonium anion and X represents Cl or Br. Thus a structural and magnetic investigation was undertaken.

$(PDA)Cu(ox)_2$ (PDA = $NH_3CH_2CH_2CH_2NH_3^{2+}$) was prepared with similar goals in mind, but the crystallographic analysis revealed a one-dimensional copper–oxalate structure.

Experimental Section

Preparation of Compounds. The compound $(BA)_2Cu(ox)_2$ was prepared by evaporation of an aqueous solution containing stoichiometric amounts of copper(II) hydroxide, oxalic acid, and benzylamine and crystallizes as pale blue platelets. Any insoluble copper oxalate that precipitated can be dissolved upon addition of an excess of benzylammonium oxalate. Royal blue crystals of $(PDA)Cu(ox)_2$ were also obtained from aqueous solution. Crystals formed when a solution containing stoichiometric amounts of copper(II) hydroxide, oxalic acid, and propylenediamine was allowed to evaporate.

X-ray Data Collection. $(BA)_2Cu(ox)_2$. The single crystal of $(BA)_2Cu(ox)_2$ used for crystallographic data collection was an eight-faceted platelet about 0.01 cm thick with a total volume of 1.25 × 10^{-5} cm^3. Systematic extinctions uniquely defined the space group as orthorhombic *Pbca*. The lattice constants, determined from a least-squares refinement on twelve well-centered reflections, are a = 7.100 (2) Å, b = 8.004 (2) Å, and c = 35.444 (8) Å. The calculated density for four molecules per unit cell is 1.11 g/cm^3.

A total of 2276 unique reflections were collected on an automated Picker four-circle diffractometer using zirconium-filtered Mo Kα radiation (λ = 0.71069 Å). A θ–2θ step scan was used with a peak width of 1.6°, step size of 0.05°, and counting of 3 s/step. Background was counted for 21 s before and after each scan. The intensities of three reflections were monitored every 40 reflections to check for decomposition, and data were corrected for linear decay and for absorption (μ = 11.8 cm^{-1}; transmission factors ranged from 0.69 to 0.89). The standard deviation of each reflection was calculated by $\sigma^2(I)$ = TC – BG + 0.03$^2I^2$, where TC is total counts, BG is background counts, and I = TC – BG.

$(PDA)Cu(ox)_2$. Data were collected for $(PDA)Cu(ox)_2$ with use of a single crystal 0.036 cm long (⟨010⟩ direction) by 0.008 cm by 0.011 cm. The monoclinic space group $C2/c$ was indicated by systematic extinctions. A least-squares refinement on 12 reflections yields a = 17.901 (3) Å, b = 4.920 (1) Å, c = 14.002 (3) Å, and β = 118.7 (2)°. For four molecules per unit cell, the calculated density is 1.94 g/cm^3.

A total of 1218 unique reflections were collected as above, except a counting time of 4 s/step was used and background was counted for 20 s before and after each scan. Absorption corrections and linear decay corrections were applied as above (μ = 18.8; transmission factors varied from 0.81 to 0.87). Linear-decay corrections were less than 5% for both salts.

Magnetic Data. The magnetic susceptibilities of both compounds were measured as powders in two different magnetometers. The first, located at Washington State University, is a PAR 155 vibrating-sample magnetometer with a calibrated carbon-glass resistance thermometer. The other, at the CNRS Laboratories, Grenoble, France, is a homemade instrument incorporating a superconducting coil capable of generating fields of 60 kOe. The Grenoble thermometer was a calibrated GaAs diode. The M vs. H curves for both compounds were

* To whom correspondence should be addressed at Washington State University.

(1) L. Dubicki, C. M. Harris, E. Kokot, and R. L. Martin, *Inorg. Chem.*, **5**, 93 (1966).
(2) B. N. Figgis and D. J. Martin, *Inorg. Chem.*, **5**, 100 (1966).
(3) K. T. McGregor and Z. G. Soos, *Inorg. Chem.*, **15**, 2159 (1976).
(4) R. W. Jotham, *J. Chem. Soc., Chem. Commun.*, 178 (1973).
(5) A. Michalowicz, J. J. Girerd, and J. Goulon, *Inorg. Chem.*, in press.
(6) J. J. Girerd, O. Kahn, and M. Verdaguer, *Inorg. Chem.*, **19**, 274 (1980).
(7) M. Melnik, M. Langfelderova, J. Garay, and J. Gazo, *Inorg. Chim. Acta*, **7**, 669 (1973); J. Garas, M. Langfelderova, G. Lundgren, and J. Gazo, *Collect. Czech. Chem. Commun.*, **37**, 3181 (1972).

0020-1669/81/1320-3308$01.25/0

Table I. Final Positional and Thermal Parameters for $(BA)_2Cu(ox)_2$

atom	x	y	z	U(1,1)	U(2,2)	U(3,3)	U(1,2)	U(1,3)	U(2,3)
Cu	0.0	0.0	0.0	0.0485 (8)	0.0328 (7)	0.0427 (8)	0.0009 (7)	0.0128 (7)	0.0022 (6)
O(1)	−0.0638 (7)	0.0703 (6)	0.0506 (1)	0.0432 (29)	0.0428 (27)	0.0464 (32)	−0.0004 (23)	0.0122 (25)	0.0052 (24)
O(2)	0.0974 (7)	0.2244 (6)	−0.0065 (1)	0.0526 (31)	0.0401 (29)	0.0444 (35)	−0.0016 (24)	0.0067 (25)	0.0007 (25)
O(3)	−0.0508 (7)	0.2992 (7)	0.0863 (1)	0.0662 (37)	0.0626 (34)	0.0430 (35)	−0.0116 (28)	0.0055 (29)	−0.0052 (29)
O(4)	0.1767 (7)	0.4385 (7)	0.0306 (1)	0.0624 (35)	0.0548 (32)	0.0512 (34)	−0.0187 (27)	0.0029 (29)	−0.0067 (28)
C(1)	−0.0144 (9)	0.2217 (9)	0.0564 (2)	0.0284 (38)	0.0553 (48)	0.0399 (45)	−0.0026 (39)	−0.0047 (34)	0.0033 (38)
C(2)	0.0970 (10)	0.3057 (9)	0.0250 (2)	0.0342 (40)	0.0391 (43)	0.0537 (52)	0.0006 (34)	0.0047 (39)	−0.0007 (40)
C(3)	0.3573 (15)	0.0771 (13)	0.1617 (3)	0.0965 (73)	0.0963 (71)	0.0538 (62)	−0.0280 (64)	0.0119 (57)	0.0058 (55)
C(4)	0.3820 (22)	0.0308 (17)	0.1998 (3)	0.1471 (124)	0.1432 (119)	0.0692 (83)	−0.0106 (98)	0.0232 (83)	0.0185 (77)
C(5)	0.5151 (21)	0.1036 (20)	0.2208 (3)	0.1113 (107)	0.1726 (141)	0.0688 (85)	0.0248 (102)	−0.0082 (82)	0.0010 (89)
C(6)	0.6238 (20)	0.2293 (20)	0.2064 (4)	0.1141 (110)	0.1713 (144)	0.0853 (97)	−0.0147 (99)	−0.0140 (84)	−0.0319 (91)
C(7)	0.6052 (15)	0.2742 (14)	0.1674 (3)	0.0885 (76)	0.1208 (90)	0.0631 (68)	−0.0097 (69)	0.0060 (62)	−0.0171 (64)
C(8)	0.4674 (10)	0.1975 (10)	0.1459 (2)	0.0439 (48)	0.0602 (48)	0.0459 (48)	0.0071 (39)	0.0100 (39)	−0.0095 (41)
C(9)	0.4372 (13)	0.2495 (11)	0.1049 (2)	0.0859 (63)	0.0933 (70)	0.0386 (52)	0.0320 (55)	0.0199 (47)	0.0013 (48)
N	0.5690 (9)	0.1490 (8)	0.0803 (2)	0.0514 (39)	0.0604 (40)	0.0396 (39)	0.0040 (33)	0.0082 (33)	−0.0044 (32)

measured at 4.2 K in fields up to 60 kOe. The benzylammonium salt curve was linear up to 35 kOe, and the PDA salt curve was linear up to 16 kOe. Magnetization vs. temperature data were collected in fields of less than 8 kOe. Corrections to the data were made for diamagnetism of the noncopper ions (BA, -212×10^{-6} emu/mol; PDA, -118×10^{-6} emu/mol). A temperature-independent paramagnetic correction (TIP) of $+60 \times 10^{-6}$ emu/mol was applied to both sets of data. Susceptibility vs. temperature data are tabulated in Tables V and VI for the benzylammonium and PDA salts, respectively. The magnetic data are believed accurate to within 1% with a precision of half that value.

Determination of Structures. $(BA)_2Cu(ox)_2$. Examination of the Patterson function gave the initial coordinates of Cu, O(1), O(2), O(3), and C(1). The rest of the atoms were located from subsequent electron density maps (except the hydrogen atoms, which were not resolved on the final difference map). Least-squares refinement of the positional and anisotropic thermal parameters of these atoms proceeded in a normal fashion. Final refinement of 1271 reflections converged to a conventional R factor ($R = \sum||F_o| - |F_c||/\sum|F_o|$) of 0.098 for all reflections and a weighted R factor ($R_w = \sum w(|F_o| - |F_c|)^2/\sum w|F_o|^2$) of 0.085. An R factor of 0.070 was achieved by omitting reflections with $F < 3.0\sigma$. The goodness of fit was 1.90 with $w = 1/\sigma^2(F)$. Maximum parameter shifts on the last cycle were about half their estimated errors. Scattering-factor tables for each atom were taken from ref 8, and the computer programs used are part of a local library.[9] Final positional and thermal parameters are tabulated in Table I, and relevant bond distances and angles are given in Table II.

(PDA)Cu(ox)$_2$. Positions of Cu, O(1), and O(2) were deduced from a Patterson synthesis. The other carbon, oxygen, and nitrogen coordinates were determined from subsequent electron density maps, and positional and anisotropic thermal parameters were refined for these atoms. Hydrogen positions were located from another difference map, and refinement of all parameters except hydrogen isotropic thermal parameters, which were fixed at 5.0, proceeded to $R = 0.085$. A conventional R of 0.037 was obtained by using only reflections with $F > 3.0\sigma$. The goodness of fit was 1.29 with $w = 1/\sigma^2(F)$. Maximum parameter shifts during the final cycle of least-squares refinement were less than one-third of their estimated errors (except for some hydrogen positional parameters). The final positional and thermal parameters are presented in Table III, while Table IV gives a tabulation of the bond distances and angles.

Structure Description

Both salts contain planar $Cu(ox)_2^{2-}$ ions in which the oxalate ions act as bidentate ligands. In each salt, the copper ions complete their coordination sphere by formation of long Cu–O bonds to noncoordinated oxygen atoms on neighboring anions. The stacking of the $Cu(ox)_2^{2-}$ anions is distinctly different in the two salts. In $(BA)_2Cu(ox)_2$, each anion interacts with four neighbors to form a definite layer structure. The benzylammonium cations separate the layers. In contrast, the anions in $(PDA)Cu(ox)_2$ form a linear chain arrangement, interacting with only two neighbors. However, the chains pack together in layers, held together by hydrogen bonds.

Table II. Bond Distances and Angles for $(BA)_2Cu(ox)_2$

atoms	dist, A	atoms	angle, deg
	Copper Coordination Sphere		
Cu-O(1)	1.933 (5)	O(1)-Cu-O(2)	85.6 (2)
Cu-O(2)	1.939 (5)	O(1)-Cu-O(4)[a]	97.2 (2)
Cu-O(4)[a]	2.586 (5)	O(2)-Cu-O(4)[a]	95.2 (2)
	Oxalate Anions		
C(1)-O(1)	1.279 (8)	O(1)-C(1)-O(3)	123.3 (6)
C(1)-O(3)	1.255 (8)	O(1)-C(1)-C(2)	116.3 (6)
C(1)-C(2)	1.522 (9)	O(3)-C(1)-C(2)	120.4 (6)
C(2)-O(2)	1.294 (8)	O(2)-C(2)-O(4)	125.2 (7)
C(2)-O(4)	1.219 (8)	O(2)-C(2)-C(1)	114.2 (6)
		O(4)-C(2)-C(1)	120.6 (7)
		C(1)-O(1)-Cu	111.2 (4)
		C(2)-O(2)-Cu	111.3 (4)
		C(2)[a]-O(4)[a]-Cu	120.7 (4)
	Benzylammonium Cation		
N-C(9)	1.510 (9)	N-C(9)-C(8)	108.5 (6)
C(9)-C(8)	1.525 (10)	C(9)-C(8)-C(3)	120.4 (8)
C(8)-C(3)	1.363 (11)	C(9)-C(8)-C(7)	120.2 (8)
C(8)-C(7)	1.384 (12)	C(3)-C(8)-C(7)	119.4 (8)
C(7)-C(6)	1.433 (15)	C(8)-C(7)-C(6)	119.0 (10)
C(6)-C(5)	1.367 (17)	C(7)-C(6)-C(5)	119.6 (11)
C(5)-C(4)	1.337 (18)	C(6)-C(5)-C(4)	120.7 (12)
C(4)-C(3)	1.409 (14)	C(5)-C(4)-C(3)	120.5 (12)
		C(4)-C(3)-C(8)	120.6 (10)
	Hydrogen Bonding		
N-O(1)	2.881 (10)		
N-O(3)	2.811 (10)		
N-O(4)	2.963 (10)		

[a] Coordinate transformed by $-1/2 + x$, $1/2 - y$, $-z$.

The anions for the two salts are shown in Figures 1 and 2, respectively. The centrosymmetric ions both have nearly D_{2h} symmetry, the anion in the benzylammonium salt showing somewhat larger distortion from ideality. The bite angles of the bidentate ligands (the O(2)–Cu–O(1) angle) are 85.6 and 85.1° for the BA and PDA salts, respectively. The interior C–C–O bond angles (113.1–116.2°) are substantially smaller than the exterior angles (119.7–120.6°) due to the steric restrictions of the planar five-member ring. The interior C–O distances (1.276–1.294 Å) are longer than the exterior distances (1.219–1.255 Å). This lengthening of 0.05 Å is due, of course, to the interaction of the interior oxygen atoms with the copper ion.

The packing of the $Cu(ox)_2^{2-}$ anions into a layer array for the BA salt is shown in Figure 3. The anions stack with the normal to the $Cu(ox)_2^{2-}$ plane lying nearly in the *ab* plane (i.e.,

(8) "International Tables for X-ray Crystallography", Vol. III, Kynoch Press, Birmingham, England, 1962, Table 3.3.1A.

(9) This includes modified versions of the following: Busing, Martin, and Levy's ORFLS least-squares program, Hubbard, Quicksall, and Jacobson's ALFF Fourier program, the function and error program ORFFE by Busing, Martin, and Levy, Johnson's ORTEP program for crystallographic illustrations, and the absorption correction subroutine ORABS by Wehe, Busing, and Levy.

Table III. Final Positional and Thermal Parameters for $(PDA)Cu(ox)_2$

atom	x	y	z	$U(1,1)$	$U(2,2)$	$U(3,3)$	$U(1,2)$	$U(1,3)$	$U(2,3)$
Cu	0.2500	0.2500	0.0	0.0168 (3)	0.0216 (3)	0.0398 (4)	0.0008 (2)	0.0097 (2)	−0.0068 (3)
O(1)	0.2936 (1)	0.5488 (5)	0.1015 (2)	0.0188 (10)	0.0288 (12)	0.0343 (12)	−0.0003 (9)	0.0069 (9)	−0.0055 (10)
O(2)	0.3609 (1)	0.1235 (5)	0.0272 (2)	0.0193 (10)	0.0276 (12)	0.0432 (13)	0.0002 (9)	0.0107 (10)	−0.0066 (11)
O(3)	0.0821 (1)	0.2969 (5)	0.5277 (2)	0.0270 (11)	0.0420 (15)	0.0398 (13)	−0.0056 (10)	0.0182 (10)	0.0025 (11)
O(4)	0.2462 (2)	0.1065 (5)	0.6610 (2)	0.0361 (13)	0.0368 (14)	0.0402 (13)	0.0019 (11)	0.0165 (11)	0.0136 (12)
C(1)	0.1433 (2)	0.4132 (6)	0.5285 (2)	0.0244 (14)	0.0268 (16)	0.0264 (15)	−0.0023 (12)	0.0120 (13)	−0.0054 (13)
C(2)	0.2350 (2)	0.3096 (6)	0.6050 (2)	0.0263 (15)	0.0250 (16)	0.0228 (14)	−0.0009 (11)	0.0096 (12)	−0.0045 (12)
C(3)	0.0	0.1647 (10)	0.2500	0.0262 (21)	0.0371 (24)	0.0240 (21)	0.0	0.0129 (19)	0.0
C(4)	0.0378 (2)	0.0132 (7)	0.6957 (3)	0.0271 (15)	0.0324 (17)	0.0257 (15)	0.0040 (13)	0.0137 (13)	0.0043 (14)
N(1)	0.0853 (2)	0.1564 (7)	0.1537 (2)	0.0257 (13)	0.0361 (15)	0.0281 (14)	0.0014 (12)	0.0150 (12)	−0.0008 (12)

atom	x	y	z	U, Å^2	atom	x	y	z	U, Å^2
H1(C3)	0.4598 (36)	0.2361 (100)	0.6837 (47)	0.0633	H4(N)	0.4517 (43)	0.2331 (112)	0.8944 (54)	0.0633
H2(C4)	0.4186 (38)	0.6573 (134)	0.7405 (47)	0.0633	H5(N)	0.3927 (39)	0.4452 (126)	0.8748 (50)	0.0633
H3(C4)	0.4936 (38)	0.6218 (127)	0.8548 (47)	0.0633	H6(N)	0.3702 (44)	0.2467 (114)	0.7951 (50)	0.0633

Table IV. Bond Distances and Angles for $(PDA)Cu(ox)_2$

atoms	dist, A	atoms	angle, deg
	Copper Coordination Sphere		
Cu-O(1)	1.931 (2)	O(1)-Cu-O(2)	94.92 (9)
Cu-O(2)	1.937 (2)	O(1)-Cu-O(4)[c]	87.70 (9)
Cu-O(4)	2.883 (3)	O(2)-Cu-O(4)[c]	86.73 (9)
	Oxalate Anions		
C(1)-O(2)	1.276 (4)	O(2)-C(1)-C(2)	114.9 (3)
C(1)-O(3)	1.230 (4)	O(3)-C(1)-C(2)	119.7 (3)
C(1)-C(2)	1.554 (4)	O(2)-C(1)-O(3)	125.4 (3)
C(2)-O(1)	1.280 (4)	O(1)-C(2)-C(1)	114.1 (3)
C(2)-O(4)	1.226 (4)	O(4)-C(2)-C(1)	120.2 (3)
		O(1)-C(2)-C(4)	125.6 (3)
		C(2)-O(1)-Cu	113.2 (2)
		C(1)-O(2)-Cu	112.7 (2)
		C(2)-O(4)-Cu	93.1 (2)
	Propylenediammonium Cation		
N(1)-C(4)	1.498 (4)	C(4)-C(3)-C(4)	109.4 (4)
C(4)[a]-C(3)	1.515 (4)	C(3)-C(4)-N(1)	110.4 (4)
	Hydrogen Bonding		
N(1)-O(3)[a]	2.829	C(4)-N(1)-O(3)[a]	87.8 (2)
N(1)-O(3)[b]	2.935	C(4)-N(1)-O(3)[b]	86.3 (2)
		O(3)[a]-N(1)-O(3)[b]	86.5 (1)

[a] Coordinates transformed by $x, -y, -1/2 + z$. [b] Coordinates transformed by $-x, y, 1/2 - z$. [c] Coordinates transformed by $1/2 - x, 1/2 + y, 1/2 - z$.

Table V. Molar Susceptibility vs. Temperature for $(BA)_2Cu(ox)_2$[a]

T, K	$10^3\chi_m$, emu/mol	T, K	$10^3\chi_m$, emu/mol	T, K	$10^3\chi_m$, emu/mol
4.82	77.9	30.2	13.5	157	2.60
5.25	71.9	32.2	12.4	168	2.42
6.00	63.5	34.2	11.6	178	2.30
6.62	58.0	37.5	10.7	187	2.18
7.65	50.4	42.5	9.45	196	2.06
8.48	45.8	48.0	8.31	207	1.96
9.44	41.5	57.8	7.00	217	1.88
10.15	38.8	61.7	6.60	227	1.81
11.18	35.7	67.5	6.03	238	1.73
12.20	32.3	77.4	5.32	249	1.65
13.75	28.7	82.9	4.95	260	1.59
14.19	27.7	87.7	4.67	270	1.53
15.46	25.7	93.3	4.34	280	1.48
16.41	24.1	98.2	4.10	290	1.46
17.61	22.6	104.4	3.89	300	1.41
19.44	20.4	108	3.76		
20.5	19.2	118	3.46		
22.9	17.4	127	3.20		
26.2	15.2	137	2.97		
27.7	14.5	147	2.78		

[a] Data corrected for diamagnetism and temperature-independent paramagnetism.

Table VI. Molar Susceptibility vs. Temperature for (PDA) for $(PDA)Cu(ox)_2$[a]

T, K	$10^3\chi_m$, emu/mol	T, K	$10^3\chi_m$, emu/mol
4.30	89.2	57.4	7.33
5.00	77.4	62.9	6.71
5.63	68.8	68.5	6.16
6.10	64.1	78.1	5.40
7.23	54.6	81.2	5.22
7.90	49.9	85.7	4.90
8.96	44.0	90.5	4.58
10.04	39.6	104.1	3.98
11.46	34.7	112.1	3.68
12.68	32.0	124.0	3.31
13.83	28.9	130.6	3.14
14.75	27.2	142.3	2.88
17.06	23.7	152.8	2.65
18.65	21.6	161.0	2.51
20.8	19.6	170.0	2.39
22.7	18.0	180.0	2.24
26.5	15.5	197.5	2.05
28.1	14.6	208.0	1.96
29.7	13.8	213.5	1.90
32.6	12.6	222.5	1.83
34.8	11.8	233.5	1.73
38.6	10.7	251	1.61
42.4	9.77	269	1.49
47.4	8.82	276	1.46
51.2	8.21	290	1.38
		300	1.32

[a] Data corrected for diamagnetism and temperature-independent paramagnetism.

within the plane of the layer of anions). This allows the O(4) atoms of each anion to bridge to a neighboring copper ion in the (110) and $(\bar{1}\bar{1}0)$ direction and, simultaneously, allows the O(4) atoms of anions in the $(\bar{1}10)$ and $(1\bar{1}0)$ directions to occupy its fifth and sixth coordination sites. Adjacent anions are not coplanar, and the C(2)–O(4)–Cu bridging angle is 120.7°. The benzylammonium ions hydrogen bond to this layer. These cations show very large thermal amplitudes of vibration, corresponding primarily to a torsional oscillation of the ion about the N–C(8) direction. The inability of a simple anisotropic vibrational ellipsoid to account for this type of motion is perhaps the major reason for the rather poor refinement of this structure.

The packing of the $Cu(ox)_2^{2-}$ anions in the $(PDA)Cu(ox)_2$ structure is easier to visualize (Figure 2). Adjacent anions are separated by unit cell translations in the b direction to form a linear chain system. Adjacent anions are thus coplanar. The O(4) oxygen atoms from neighboring anions again complete the coordination sphere of the copper ions, the C(2)–O(4)–Cu angle now being 93.1°. The ammonium groups of the PDA

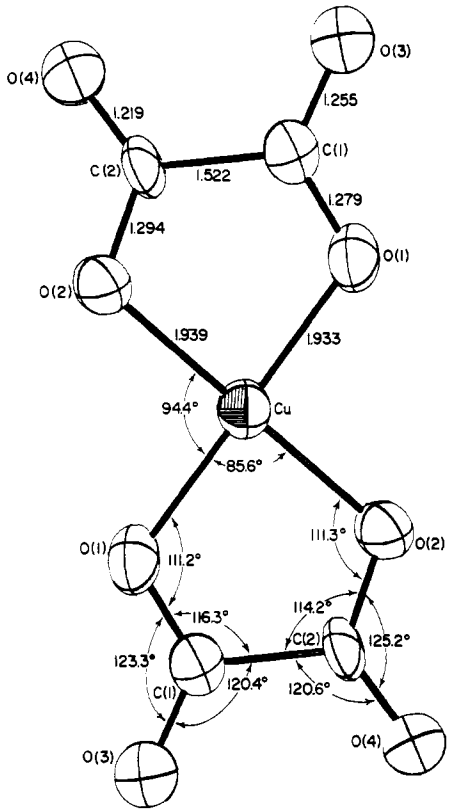

Figure 1. The $Cu(ox)_2^{2-}$ anion in $(BA)_2Cu(ox)_2$.

ions hydrogen bond the chains together in the *c* direction (Figure 4), forming sheets in the *bc* plane. The PDA ions themselves lie between adjacent sheets.

Analysis of Magnetic Data

$(BA)_2Cu(ox)_2$. The susceptibility data for $(BA)_2Cu(ox)_2$ above 150 K were fit to a Curie–Weiss relation; the parameters determined were $C = 0.419$, $g = 2.11$, and $\Theta = -4$ (1) K, indicating dominant antiferromagnetic interactions. Due to the two-dimensionality of the Cu oxalate layers, further analysis was restricted to lower-dimensional models. The data from 4.8 to 300 K were fit to the theoretical predictions for the susceptibility of a two-dimensional, $S = {}^1/_2$ antiferromagnet with Heisenberg exchange interaction, $\mathcal{H} = -2J\sum S_i S_j$. There are several expressions for this susceptibility available in the literature. One is due to Baker et al.[10] and is a high-temperature series expansion for the susceptibility in terms of powers of J/kT; another is due to Lines[11] and is an expansion for the reciprocal susceptibility based upon the coefficients determined by Rushbrooke and Wood. The J defined by Lines is equal to $2J$ of Rushbrooke and Wood and Baker.[12] Both expressions yielded the same values for the two fitting parameters J/k and g: $J/k = -0.21$ (1) K, $g = 2.09$ (1). Good agreement between the data and the predicted susceptibility is obtained with these parameters over the whole temperature range as can be seen in Figure 5.

$(PDA)Cu(ox)_2$. The magnetic data for $(PDA)Cu(ox)_2$ are plotted in Figure 6 as $\chi_m T$ vs. temperature. The initial rise in $\chi_m T$ with decreasing temperature indicates a dominant ferromagnetic interaction. A Curie–Weiss plot of the data above 170 K yields values for C (g) and Θ of $C = 0.398$ ($g = 2.059$) and $\Theta = +3.5$. However $\chi_m T$ reaches a maximum of 0.423 emu K/mol near 72 K and then descends gradually. Such a turnover indicates weaker antiferromagnetic interactions are also present in the material.

As a first attempt, the high-temperature data ($T > 80$ K) were fit to the prediction for the susceptibility of a linear chain of Heisenberg-coupled $S = {}^1/_2$ atoms[13] with an antiferromagnetic parameter introduced with the molecular-field corrected formula[14]

$$\chi_m(\text{cor}) = \chi_m/[1 - (z'J'/Ng^2\mu_B{}^2)\chi_m]$$

(The use of such a correction to account for interchain effects in the one-dimensional $S = {}^1/_2$ ferromagnetic compounds $CuCl_2X$ ($X = Me_2SO$, Me_4SO)[15a] has been justified by single-crystal magnetic studies.[15b] In these salts, $|J'/J| \sim (2\text{–}4) \times 10^{-2}$.) When the data are fit from 40 to 300 K (the maxima appears near 72 K), a moderately good fit is obtained with parameters $J/k = 15.8$ K and $z'J' = -17.7$ K. The agreement is probably fortuitous since the molecular field approximation is invalid when $J' \sim J$.

These results, coupled with the structural characteristics of the $(PDA)Cu(ox)_2$, make it reasonable to interpret the magnetic behavior in terms of a rectangular two-dimensional network, with the dominant, ferromagnetic (J) interactions within the chains and a secondary, antiferromagnetic interaction (J') between the chains in the *c* direction. The theoretical analysis of the susceptibility of such a model is complex, and results have only been recently obtained[16,17] for the special cases of the $S = \infty$ Heisenberg, $S = \infty$ XY, and $S = {}^1/_2$ Ising rectangular models. The desired $S = {}^1/_2$ Heisenberg model appropriate for a lattice of copper ions has not been dealt with theoretically. As an initial analysis of the susceptibility of $(PDA)Cu(ox)_2$, one of the three extant models must be used; we have chosen to use the $S = {}^1/_2$ Ising model for reasons given below.

The theoretical expressions for the susceptibilities of the rectangular magnets have been calculated with use of a new calculational technique. A two-dimensional magnetic lattice consisting of $(N + 1) \times (N + 1)$ spins is decomposed into $(N + 1)$ interacting linear chains. The susceptibility is then expressed in powers of (J'/kT) whose coefficients are given by many-spin correlation functions within the linear chain, where J' is the interchain exchange constant. The many-spin correlation function can be calculated exactly for linear-chain $S = \infty$ Heisenberg, $S = \infty$ XY, and $S = {}^1/_2$ Ising models. From the calculation of terms out to third order in (J'/kT), expressions for the susceptibilities for square-planar $S = \infty$ Heisenberg,[16] $S = \infty$ XY,[17] and $S = {}^1/_2$ Ising[17] models are found. The expression for the $S = {}^1/_2$ square-planar Ising model is

$$\chi = (Ng^2\mu_\beta{}^2/k_0T)[A_0(T) + A_1(T)K' + A_2(T) \times (K')^2 + A_3(T)(K')^3 + \ldots]$$

where

$$K' = J'/2kT$$
$$A_0(T) = (1 + U)/(1 - U)$$
$$A_1(T) = 2A_0(T)^2$$
$$A_2(T) = 2A_0(T)^3 + 4U(1 + U + U^2)/[(1 + U)(1 - U)^3]$$
$$A_3(T) = 4[U^4 + 12U^3 + 16U^2 + 12U + 1]/[3(1 - U)^4]$$

(10) G. A. Baker, H. E. Gilbert, J. Eve, and G. S. Rushbrooke, *Phys. Lett. A*, **25A**, 207 (1967).
(11) M. E. Lines, *J. Phys. Chem. Solids*, **31**, 101 (1970).
(12) G. S. Rushbrooke and P. J. Wood, *Mol. Phys.*, **1**, 257 (1958).
(13) G. A. Baker, G. S. Rushbrooke, and H. E. Gilbert, *Phys. Rev.* [*Sect.*] *A*, **135**, 1272 (1964).
(14) R. L. Carlin and A. J. van Duyneveldt, "Magnetic Properties of Transition Metal Compounds", Springer-Verlag, New York, Heidelberg, Berlin, 1977, p 139.
(15) (a) D. D. Swank, C. P. Landee, and R. D. Willett, *Phys. Rev. B: Condens. Matter*, **26**, 2154 (1979); (b) C. P. Landee and R. D. Willett, *J. Appl. Phys.*, **52**, 2240 (1981).
(16) K. Katsumata, *Solid State Commun.*, **23**, 481 (1977).
(17) K. Katsumata and T. Tonegawa, *Solid State Commun.*, **25**, 925 (1978).

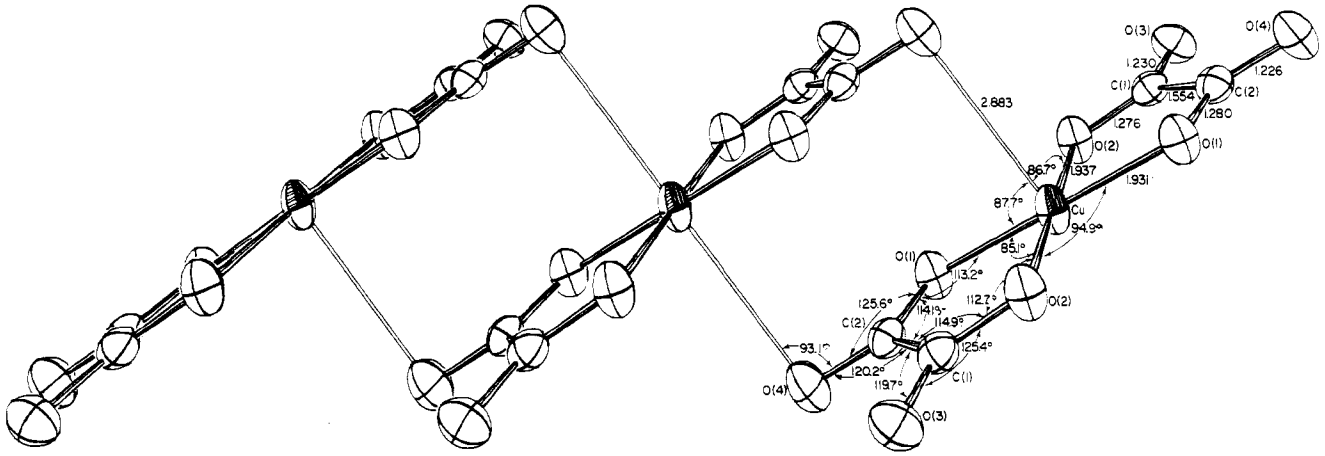

Figure 2. View of the $Cu(ox)_2^{2-}$ anion in $(PDA)Cu(ox)_2$ showing the stacking of the anions parallel to the b direction.

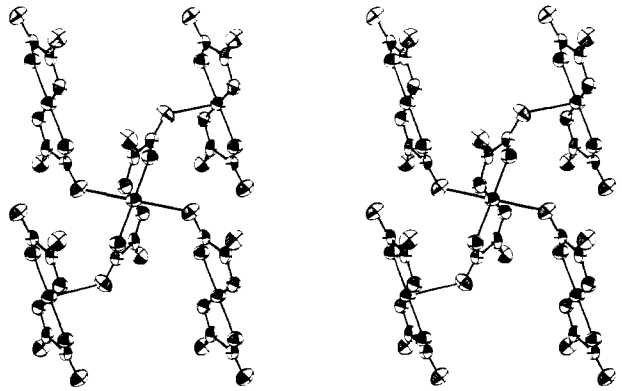

Figure 3. Stereographic view of the layer of $Cu(ox)_2^{2-}$ anions in $(BA)_2Cu(ox)_2$ from the c direction. The a axis is horizontal, and the b axis is vertical.

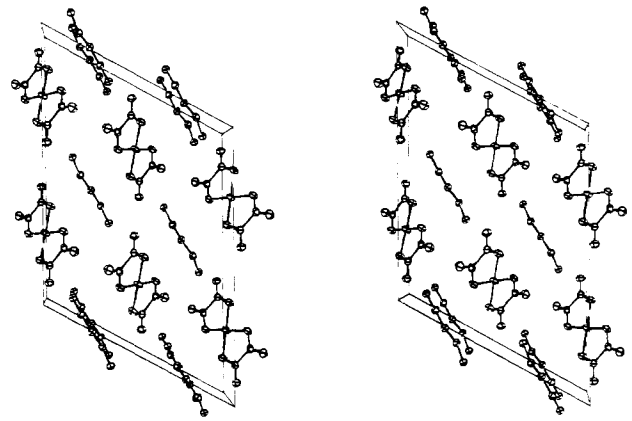

Figure 4. Stereographic view of the unit cell contents of $(PDA)Cu(ox)_2$ from the b direction (looking down the chain axis). The a axis is vertical.

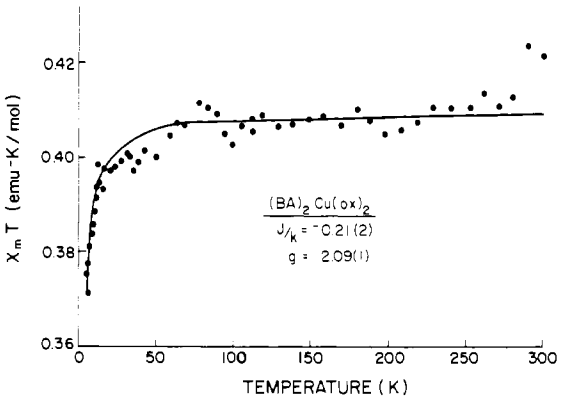

Figure 5. Molar susceptibility times temperature vs. temperature for $(BA)_2Cu(ox)_2$. The solid curve is the theoretical least-squares fit.

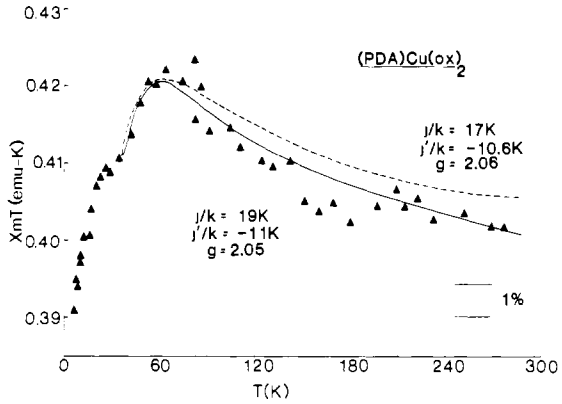

Figure 6. Molar susceptibility times temperature vs. temperature for $(PDA)Cu(ox)_2$. The solid line is the theoretical fit; the dashed curve is the fit as described in the text.

where $U = \tanh(J/2kT)$. Note that Katsumata and Tonegawa[17] used an interaction Hamiltonian of the type $\mathcal{H} = -2J\sum\sigma_i\sigma_j$ with σ the Pauli spinors. The above expression has replaced the original J and J' by $J/4$ and $J'/4$ in order to give the proper behavior based upon the interaction Hamiltonian $\mathcal{H} = -2J\sum S_i^z S_{i+1}^z$.

Since the expression for the susceptibility of the rectangular models is based upon the appropriate linear chain results, the decision of which model to use as an approximation to the susceptibility of the $(PDA)Cu(ox)_2$ is based upon a comparison of the susceptibility of the $S = {}^1/_2$ Heisenberg linear chain to that of the $S = {}^1/_2$ Ising and $S = \infty$ Heisenberg and XY chains. In the high reduced temperature range, T^* ($\equiv kT/J$) > 4, the $S = {}^1/_2$ Ising model susceptibility differs less than 3% from that of the $S = {}^1/_2$ Heisenberg model and is a better approximation than the classical spin models. It thus seemed appropriate to fit the susceptibility data for $(PDA)Cu(ox)_2$ to the model of the anisotropic $S = {}^1/_2$ two-dimensional Ising model of Katsumata and Tonegawa. Good agreements were found when three-parameter fits (J/k, J'/k, and g) were used. It was noted, however, that the best-fit parameters depended on which temperature range was being considered. When data exclusively above the maxima in $\chi_m T$ were used, both J and J' were found to be ferromagnetic. Incorporating lower temperature data forced J' to be antiferromagnetic. A least-squares fit to the data was made with only data above 40 K included. With g fixed at 2.06, the best-fit parameters were

found to be J/k = 16.2 K and J'/k = −10.0 K; with g = 2.05, they were J/k = 19.0 and J'/k = −11.0 K. The theoretical curve is plotted as the solid curve in Figure 6. It was recognized that the two parameters could be fit independently, with g held constrained to a value of 2.06. The maximum value of $\chi_m T$ predicted by the model depends only on the ratio $|J'|/J$, while, for a given ratio, the temperature at which the maximum occurs is determined by J. With use of this procedure, the dashed theoretical curve shown in Figure 6 was obtained with J/k = 17 (1) K, $|J'|/J$ = 0.62 (2) (i.e., J'/k = −10.6 (3) K), and g = 2.06. Agreement is reasonable above 30 K. Deviations below that temperature are attributed to the inappropriateness of the Ising model to this compound. The results from the three calculations (mean field, $\chi_m T$ maximum, and least squares) are in reasonable agreement.

The susceptibility data for $(PDA)Cu(ox)_2$ is thus reasonably accounted for in terms of a rectangular $S = {}^1/_2$ Ising model. Such a model has been used in spite of the limitations described above in the absence of a more appropriate model. Nevertheless, the value of the ferromagnetic exchange constant within the chains can be evaluated relatively precisely since it is determined by the high-temperature behavior where the limitations of the model are least significant. We thus consider the ferromagnetic exchange constant to be relatively well determined as 19 (2) K. Since a change of g of 0.01 alters the best-fit value of J/k = +3 K, no greater value can be attributed to the exchange constant. The exchange between the chains can be less well determined since it influences the behavior of the susceptibility at lower relative temperatures where the inappropriateness of the Ising model becomes apparent. For a J/k of 19 K reasonable agreement (<3%) between the Ising and Heisenberg models only occurs above 90 K. Below this temperature, the Ising model will predict divergence of χ_m for the linear chain considerably faster than the more appropriate (but unavailable) Heisenberg model. In order to force $\chi_m T$ to turn over, the antiferromagnetic J' is necessary. It is important to recognize that J' must be overestimated in order to compensate for the excessive ferromagnetic chain susceptibility. The value of $|J'/k|$ obtained (11 K) is thus too large; how much too large is difficult to estimate without a more quantitative theory.

Discussion

The structures of $(BA)_2Cu(ox)_2$ and $(PDA)Cu(ox)_2$ present two new structural systems for magnetic studies. $(BA)_2Cu(ox)_2$ is a weakly coupled two-dimensional antiferromagnet. This structural type is expected to be stable for $(RNH_3)_2Cu(ox)_2$ systems whenever R is a relatively bulky group. In contrast, $(PDA)Cu(ox)_2$ forms a strongly coupled one-dimensional ferromagnetic system; however, there is very strong interchain coupling. The generality of this lattice type is not known, but it seems reasonable to assume it will exist for most aliphatic ammonium ions.

It is interesting to compare these two structures with those of $K_2Cu(ox)_2 \cdot 2H_2O$ and $Na_2Cu(ox)_2 \cdot 2H_2O$. The former[18] contains chains of $Cu(ox)_2^{2-}$ anions. Half of the ions complete their coordination by bridging to a terminal oxygen (O(4) in our notation) on each of two adjacent anions; the remainder of the ions complete their coordination with water molecules. This chain may be visualized as a ribbon cut along a 110 direction from the layers present in $(BA)_2Cu(ox)_2$ (see Figure 3), with water molecules replacing oxalate ions from adjacent ribbons. Thus it is easy to visualize formation of the $(BA)_2Cu(ox)_2$ lattice upon dehydration of the $K_2Cu(ox)_2 \cdot 2H_2O$ lattice. Weak antiferromagnetic coupling exists along the chains.[19] The sodium salt[20] has chains composed of parallel stacks of $Cu(ox)_2^{2-}$ anions. However, the stacking is such that a coordinated oxygen (O(1) in our notation) on adjacent anions occupies the fifth and sixth coordination sites. Thus, the repeat distance along the chain is only 3.576 Å, in contrast to 4.920 Å in $(PDA)Cu(ox)_2$. In spite of this, the exchange interaction along the chain is only J/k = −1.7 K.[20a] The authors argued that this was the result of a δ-type overlap of magnetic orbitals. Our results effectively refute that assertion, since such overlap cannot occur in the $(PDA)Cu(ox)_2$ structure.

The existence of ferromagnetic intrachain interactions in $(PDA)Cu(ox)_2$ is extremely interesting in light of recent studies on $S = {}^1/_2$ linear chain systems with ferromagnetic interactions. Materials of this type are important theoretically and experimentally since they represent the simplest magnetic systems with extended interactions.[21] The first such system, $[(CH_3)_3NH]CuCl_3 \cdot 2H_2O$, was reported by Carlin.[22] This salt had a small exchange constant, $J/k \sim 0.85$, with rather poor isolation of the chains ($|J'/J| \sim 10^{-1}$). In our laboratory, we have synthesized a large series of these systems with large J values ($J/k > 30$ K) and varying ratios of $|J'/J|$ ranging from $\sim 10^{-4}$ up to 10^{-1}.[15,20-23] Those include $CuCl_2 \cdot Me_4SO$,[15] $CuCl_2 \cdot Me_4SO$,[15] $[(CH_3)_4N]CuCl_3$,[23] $[(CH_3)_3NH]_3Cu_2Cl_7$,[23] $(C_6H_{11}NH_3)CuCl_3$,[24] $(C_6H_{11}NH_3)CuBr_3$,[25] $(C_5H_9NH_3)CuCl_3$,[25] and $[(CH_3)_2CHNH_3]CuCl_3$.[26] These systems are proving very valuable in probing many of the properties of ferromagnetic one-dimensional systems with nearly Heisenberg-type exchange interactions. However, the large J values preclude using them to probe the low-dimensional EPR behavior since spin anisotropies dominate the relaxation processes. Similarly, the small J value for $[(CH_3)_3NH]CuCl_3 \cdot 2H_2O$[22] makes it less than ideal for probing spin dynamics. The linear-chain system found in $(PDA)Cu(ox)_2$ then, with its intermediate J value of J/k = 19 K, would be an attractive system for EPR studies if cations could be found that could stabilize the linear chain structure while simultaneously increasing the interchain interactions.

The ferromagnetic coupling in $(PDA)Cu(ox)_2$ is a direct result of the parallel stacking of the anions with O(4) essentially directly above the adjacent copper ion. Thus there is no interaction between the σ-electron systems of neighboring anions. The principal superexchange pathway can be envisioned as through the Cu d_{z^2} interaction with the neighboring anion. With the C(2)–O(4)–Cu bond angle only slightly greater than 90° (actually 93.1°), the overlap of the d_{z^2} orbital will be primarily with the oxalate π system, and it will be nearly orthogonal to the σ system. Thus, ferromagnetic coupling is to be anticipated. In contrast, the nonparallel stacking and larger C(2)–O(4)–Cu angle in $(BA)_2Cu(ox)_2$ will lead to more interaction between the d_{z^2} orbital and the σ system of the adjacent anion. Thus, a stronger antiferromagnetic contribution to the exchange is predicted. In fact, that interaction should be "tunable" by varying the bulk of the cation, with the interaction becoming more antiferromagnetic as the cation bulk increases.

In conclusion, two new magnetic systems have been synthesized and characterized. In both, potential for expansion into a series of systems with interesting magnetic properties

(18) M. A. Viswamitra, *J. Chem. Phys.*, **37**, 1408 (1962).
(19) D. Y. Jeter and W. E. Hatfield, *Inorg. Chim. Acta*, **6**, 523 (1972).
(20) (a) A. Gleizes, F. Maury, and J. Galy, *Inorg. Chem.*, **19**, 2074 (1980); (b) P. Chananont, P. E. Nixon, J. M. Waters, and T. N. Waters, *Acta Crystallogr., Sect. B*, **B36**, 2145 (1980).
(21) J. C. Bonner, *J. Magn. Magn. Mater.*, **15–18**, 1003 (1980).
(22) H. A. Algra, L. J. de Jongh, H. W. J. Blote, W. J. Huiskamp, and R. L. Carlin, *Physica B+C (Amsterdam)*, **78B+C**, 314 (1974).
(23) C. P. Landee and R. D. Willett, *Phys. Rev. Lett.*, **43**, 463 (1979).
(24) R. D. Willett, C. P. Landee, R. M. Gaura, D. D. Swank, H. Groenendijk, and A. J. van Duyneveldt, *J. Magn. Magn. Mater.*, **15–18**, 1055 (1980); H. Groenendijk, H. W. J. Blöte, A. J. van Duyneveldt, R. Gaura, C. P. Landee, and R. D. Willett, *Physica*, **B106**, 47 (1981).
(25) R. M. Gaura, C. P. Landee, and R. D. Willett, to be submitted for publication.
(26) S. A. Roberts, D. R. Bloomquist, R. D. Willett, and H. W. Dodgen, *J. Am. Chem. Soc.*, **103**, 2603 (1981).

clearly exists. With bulky cations, we anticipate obtaining two-dimensional antiferromagnets, with variable values of exchange constants. With smaller cations, linear-chain salts with moderately strong ferromagnetic intrachain interactions are anticipated. The challenge here will be to synthesize similar salts with much smaller interchain interactions ($|J'/J| < 10^{-2}$).

Acknowledgment. C.P.L. thanks the Groupe des Transitions de Phases, CNRS, Grenoble, particularly C. Schlenker and B. K. Chakraverty, for their generous hospitality during his stay with them. We also acknowledge the help of Professor H. Arend, Festkörperphysik, ETH, Zurich, in developing techniques of preparing the $(BA)_2Cu(ox)_2$ salt.[27] This work was supported by the National Science Foundation.

Registry No. $(BA)_2Cu(ox)_2$, 78307-65-0; $(PDA)Cu(ox)_2$, 78307-66-1.

(27) R. D. Willett, H. Arend, and M. Ehrensperger, *J. Cryst. Growth*, **53**, 437 (1981).

Contribution from the Department of Chemistry, Rutgers, The State University of New Jersey, New Brunswick, New Jersey 08903

Magnetic Properties of $K_5[(H_2O)_3(SO_4)_6Fe_3O]\cdot 6H_2O$, a Sulfate Analogue of the Trimeric Basic Iron(III) Carboxylates

JOHN A. THICH, BRIAN H. TOBY, DANA A. POWERS, JOSEPH A. POTENZA,* and HARVEY J. SCHUGAR*

Received August 21, 1980

The title complex contains isolated $[(H_2O)_3(SO_4)_6Fe_3O]^{5-}$ clusters with triangular-planar Fe_3O units bridged by sulfate groups. The effective magnetic moment per Fe(III) in this antiferromagnetic complex varies from 3.40 μ_B at 299.6 K to 2.05 μ_B at 85 K and agrees well with that predicted by the triangular cluster model ($H = -2J(S_1\cdot S_2 + S_1\cdot S_3 + S_2\cdot S_3)$) with $g = 2.00$, TIP = 0, $S_1 = S_2 = S_3 = {}^5/_2$, and $J = -26.0$ cm^{-1}. Since significant Fe(III)···Fe(III) magnetic coupling via bridging SO_4^{2-} appears to be small and comparable magnetic behavior ($J \simeq -30$ cm^{-1}) has been reported for several carboxylate-bridged analogues, the antiferromagnetism shown by these clusters originates either exclusively or predominantly in the Fe_3O^{7+} unit. The structural and magnetic features of Fe_3O^{7+}, Fe_2O^{4+}, and $Fe_2(OH)_2^{4+}$ clusters are compared and discussed. The extent of antiferromagnetism in these clusters appears to be related to the length of the Fe–O bond(s) in the bridge(s). Of lesser importance are variations in the Fe–O–Fe or Fe–OH–Fe bridging angles and in the nature of the nonbridging ligands.

Introduction

Oxygen-bridged Fe(III) clusters play an important role in the inorganic and bioinorganic chemistry of Fe(III).[1-3] Consequently, the properties of such species have received considerable attention, and complexes containing both Fe_2O^{4+} (linear[4] and nonlinear[5]) and $Fe_2(OR)_2^{4+}$ (R = H, alkyl)[6] units have been characterized electronically, structurally, and magnetically. The triangular Fe_3O^{7+} unit, found in the trimeric basic Fe(III) carboxylates, has also been characterized structurally.[7,8]

A basic Fe(III) sulfate, known from early work[9] as Maus' salt (synthetic material) or metavoltine (natural material), has been shown to crystallize in the hexagonal system. Synthetic material, formulated as $K_5[(H_2O)_3(SO_4)_6Fe_3O]\cdot 7H_2O$, has been shown[10] to contain crystallographically equivalent Fe(III) ions in $[(H_2O)_3(SO_4)_6Fe_3O]^{5-}$ trimeric units with bridging sulfate groups. Based on its structure, this uniaxial complex appears to be well suited for electronic–structural and magnetic studies, particularly since, relative to carboxylate, bridging SO_4^{2-} is spectroscopically transparent and since Fe(III) superexchange coupling via bridging SO_4^{2-} appears to be modest. We report here the characterization of the $[(H_2O)_3(SO_4)_6Fe_3O]^{5-}$ unit by magnetic susceptibility measurements and by single-crystal electronic spectral studies.

Experimental Section

1. Preparation and Characterization of the Title Complex (1). The preparation of **1** by concentrating aqueous $Fe_2(SO_4)_3/K_2SO_4$ at 80 °C has been described elsewhere.[9-11] Our procedure employs a lower temperature and the addition of K_2CO_3. All chemicals employed were reagent grade products of the J. T. Baker Co. A hot solution of 27.0 g of hydrated $Fe_2(SO_4)_3$ (71.8% assay as $Fe_2(SO_4)_3$ by standard EDTA

(1) Spiro, T.; Saltman, P. *Struct. Bonding (Berlin)* **1969**, *6*, 115-156.
(2) Gray, H. B.; Schugar, H. J. "Inorganic Biochemistry"; Eichhorn, G., Ed.; American Elsevier: New York, 1973; Chapter 3.
(3) Webb, J. "Techniques and Topics in Bioinorganic Chemistry"; McAuliffe, C. A., Ed.; Wiley: New York, 1975; Chapter 4.
(4) Ou, C. C.; Wollmann, R. G.; Hendrickson, D. N.; Potenza, J. A.; Schugar, H. J. *J. Am. Chem. Soc.* **1978**, *100*, 4717-4724.
(5) Murray, K. S. *Coord. Chem. Rev.* **1974**, *12*, 1-35.
(6) Ou, C. C.; Lalancette, R. A.; Potenza, J. A.; Schugar, H. J. *J. Am. Chem. Soc.* **1978**, *100*, 2053-2057.
(7) Holt, E. M.; Holt, S. L.; Tucker, W. F.; Asplund, R. O.; Watson, K. J. *J. Am. Chem. Soc.* **1974**, *96*, 2621-2623.
(8) Anzenhofer, K.; DeBoer, J. J. *Recl. Trav. Chim. Pays-Bas* **1969**, *88*, 286-288.
(9) (a) Grossner, B.; Arm, M. *Z. Kristallogr., Kristallgeom., Kristallphys., Kristallchem.* **1930**, *72*, 202-236. (b) Mellor, J. W. "A Comprehensive Treatise on Inorganic and Theoretical Chemistry"; Longmans, Green and Co.: New York, 1935; Part 3, pp 339, 341. (c) "Gmelins Handbuch der Anorganischen Chemie"; Springer-Verlag: Berlin, 1932; Vol. 59, Iron Compounds, Chapter B, pp 932, 1018.
(10) Giacovazzo, C.; Scordari, F.; Menchetti, S. *Acta Crystallogr., Sect. B* **1975**, *B31*, 2171-2173.

0020-1669/81/1320-3314$01.25/0